BRIEF COMMUNICATION

Impulsivity is associated with firing regularity in parkinsonian ventral subthalamic nucleus

Matteo Vissani[1,2], Federico Micheli[1,2], Guido Pecchioli[3], Silvia Ramat[3] & Alberto Mazzoni[1,2]

[1]The Biorobotics Institute, Scuola Superiore Sant'Anna, Pisa, 56025, Italy
[2]Department of Excellence in Robotics and AI, Scuola Superiore Sant'Anna, Pisa, 56025, Italy
[3]AOU Careggi, Dipartimento Neuromuscolo-Scheletrico e degli Organi di Senso, Florence, Italy

Correspondence
Alberto Mazzoni, The Biorobotics Institute of Scuola Superiore Sant'Anna, Viale Rinaldo Piaggio 34, Pontedera, Pisa, Italy. Tel: +39 050 883420; Fax: +39 050 883497; E-mail: alberto.mazzoni@santannapisa.it

Received: 27 October 2021; Revised: 28 January 2022; Accepted: 14 February 2022

***Annals of Clinical and Translational Neurology* 2022; 9(4): 552–557**
doi: 10.1002/acn3.51530

Matteo Vissani and Federico Micheli share the same first-author contribution.

Abstract

Impulsive–compulsive behaviors (ICB) are over-represented in Parkinson's disease (PD) patients. Neurons in the ventral subthalamic nucleus (STN) might play a predominant role in the modulation of impulsivity. We characterized the firing regularity of 742 subthalamic neurons from 24 PD patients (12 ICB+ and 12 ICB-) in an OFF medication state. We computed the firing regularity in the dorsal and ventral STN regions, and we compared their performance in discriminating ICB patients. Regularity of ventral neurons in ICB+ patients is higher and supports a significant discrimination between the two cohorts. These results substantiate a ventral location of neurons involved in impulsivity.

Introduction

Parkinson's disease (PD) patients following dopamine replacement therapies display an excess prevalence of impulsive–compulsive behaviors (ICB),[1] but the underlying neural dynamics is not completely clear. Subthalamic nucleus (STN) activity is known to affect decisional impulsivity[2,3] and several results point toward a specific involvement of the ventral subregion, which is functionally connected to the prefrontal cortex.[4,5] Theta-alpha local field potential (LFP) oscillations characterizing the ventral STN[5,6] correlate with Barrat impulsiveness scale (BIS)[7] and are particularly strong in ICB PD patients in drugs ON state.[8] Deep brain stimulation (DBS) on STN alters impulsivity in simple tasks,[9,10] especially when the target is in the ventral part.[4,11] Microelectrode recording (MER) studies on STN single neuron activity showed a relationship with decision-making and ICB[12] but did not investigate how this relationship varied within the STN. Recently, we observed in PD ICB subjects in drugs OFF condition a significant reduction in standard PD markers in STN single unit activity such as beta oscillations and burstiness.[13] Here, we investigate whether this ICB-specific feature can be associated to a specific location within STN.

Patients and Methods

Patients

This study was conducted in accordance with the Declaration of Helsinki and after ethical approval of the committee of Careggi Hospital (Florence, Italy) where all patients were operated. We retrospectively considered 32 consecutively acquired patients, 16 of whom were diagnosed with at least one current ICB. From this set, we selected the recordings in which the number of neurons identified in MER was sufficient to perform a depth-wise analysis (see below).[13] The final dataset included 24 patients, 12 of whom with ICB. The two subgroups (ICB− vs. ICB+) differed significantly only on the Barratt impulsiveness scale (see Table 1).

Surgical procedure and electrophysiological recordings

A stereotactic frame-based procedure with intraoperative MER and macrostimulation for STN targeting was used for surgery. Anatomical localization of the STN was performed using T2, SWI, and T1 sequences of the preoperative 1.5-T MRI fused with preoperative stereotactic CT

Table 1. Patient demographic details and clinical characteristics of the two cohorts.

	Gender (M)	Age at DBS (years)	Disease duration (years)	UPDRS-III OFF	L-dopa- equivalent dose LEDD (mg/day)	Dopa agonist LEDD (mg/day)	phenotype (bradykinetic-rigid / tremor dominant)	Barrat impulsiveness scale (BIS)
Parkinson's disease ICB + n = 12	8	61.5 [57.7–65.3]	14.0 [11.1–16.9]	25.5 [21.7– 29.3]	1050.0 [832.8–1267.2]	420 [140–535] 9/12	7/5	66.5 [63.9–69.1]
Parkinson's disease ICB - n = 12	9	62.5 [60.3–64.7]	11.0 [9.3– 12.7]	37.0 [32.8– 41.2]	1235.0 [1061.4–1408.6]	320 [160–1070] 9/12	6/6	54.5 [53.2– 55.8]
Test, significance ICB - vs. ICB +	Fisher Exact test, $p = 0.99$	Unequal variance T-test, $t(22) = 2.05$, $p = 0.06$	T-test, $t(22) = -0.73$, $p = 0.47$	T-test, $t(22) = 1.98$, $p = 0.06$	T-test, $t(22) = 0.57$, $p = 0.58$	Mann–Whitney *U* test, $p = 0.9$	Fisher exact test $p = 0.9$	T-test, $t(22)$, $t = 7.61$, $p < 0.001$***

Asterisks indicate the statistical significance: *p*-value < 0.05*, < 0.01**, and < 0.001***.

scan (with Leksell G frame) assisted by StealthStation (Medtronic Inc., Minneapolis, MN). The implantation of quadripolar DBS electrodes (model 3389; Medtronic) was performed bilaterally, under local anesthesia (2% lidocaine and bupivacaine). Electrophysiological recordings were performed using a Medtronic lead-point system, starting at 10 mm above the target location identified by stereotactic imaging. An exploratory trajectory was followed by extruding the microelectrode (250 lm tip, impedance 1–1.5 MX; FHC Inc., Bowdoinham ME) for each insertion. Recordings were performed with steps of 0.5 mm along three parallel traces (anterior, central, and lateral) with a 2-mm lateral spacing. Each recording lasted at least 10 seconds. Signals were sampled at 24 kHz and high-pass filtered with a hardware filter at 200 Hz to allow for a better visualization of firing neuronal activity during surgery. Afterward, an implanted pulse generator was fixed to the DBS electrodes under general anesthesia. Post-surgery imaging was performed to ensure that the electrode was in the STN.

STN entry point and subregions identification

First, every recording in which more than 50% of the total duration of the signal was visually identified as noisy was discarded. Then, for each insertion, the recordings performed within STN were identified as those exceeding the 80th percentile of activity,[14] as in previous works.[13] In total, we selected 548 STN recordings which were used for the analysis. We expressed the anatomical location of the recordings as normalized depths using the STN boundaries defined through electrophysiology within that trajectory where 0 and 1 represent the dorsal STN entrance and the ventral STN exit, respectively. No selection based on the trace position (anterior, central, and lateral) was performed.

Spike detection and neural marker estimation

Single-unit activity (SUA) was sorted using MATLAB ToolBox WaveClus. We extracted 742 SUA (330 SUA in the ICB- group and 412 in the ICB+ group) from 548 recordings across all subjects. For each SUA we fitted the interspike interval histogram with a Gamma distribution and we determined the associated parameter log(k). This shape factor was adopted as measure of firing regularity.[15]

Classification performance

We built a 5-folds Support Vector Machine (SVM) classifier using the single-subject averaged shape factor to

classify ICB- and ICB+ patients. We characterized the classifier performance in terms of accuracy, sensitivity, specificity, and area under the receiver operating characteristic curve (AUC).

Statistical analysis

We used a linear mixed model (LMM) to analyze the interaction between normalized depths (dorsal vs. ventral divided by 0.5 depth) and impulsivity with the patient as random effect (*lme* R package). Post hoc tests have been Tukey's HSD corrected (*multcomp* R package). We computed mutual information between irregularity and impulsivity.[15] Permutation test was adopted to assess the information significance. All analyses have been carried out splitting neurons in more dorsal and ventral relative to a reference normalized depth ranging from 0.3 to 0.7 (0.5 if not explicitly mentioned). We tested impulsive-domain specificity of our results repeating all the analyses in two new patients' cohorts created median-splitting the motor severity according to the UPDRS scale (UPDRS- and UPDRS+). Data are expressed as Median [Median-IQR/$\sqrt{N}$ Median + IQR/$\sqrt{N}$]. For accuracy, brackets report the 95% confidence interval computed by the Clopper–Pearson method (*binofit* in Matlab).

Results

Neurons in the ventral part of ICB+ patients are significantly more regular and less bursty (as measured by log (k), see Methods) than those of ICB- patients, while this difference is not present in the dorsal part, in which neurons display irregular behavior for both conditions (LMM, factors depth and ICB condition, interaction $p < 0.01$). Firing regularity was found to be independent from motor severity (LMM, factors depth and ICB condition, interaction $p = 0.24$). Firing regularity in the ventral part of STN carried significant information about ICB condition (0.016 Bits, bootstrap test $p < 0.05$). No information about ICB condition was carried by regularity in the dorsal part (0.003 Bits, bootstrap test $p = 0.63$). No information about UPDRS level was carried by regularity in the dorsal or the ventral part (0.006 Bits, 0.004 Bits, bootstrap test $p = 0.89$).

In the previous analysis, dorsal and ventral parts were divided with a median split. However, the result is robust to the selected partition between dorsal and ventral part. The difference in regularity between ICB+ and ICB- conditions increased when we considered neurons in more ventral parts and was significant for all depths higher the median split (Figure 1A, $p < 0.01$). The way log(k) depended on depth led to an increase of information content relatively to condition (Figure 1C, $p < 0.05$ for all depth splits >0.4). For no depth the regularity displayed significant differences between high and low UPDRS (Figure 1B,D).

We then developed a SVM algorithm (see Methods) to discriminate between ICB+ and ICB- patients based on the regularity of neurons recorded during each implant. Decoding based on dorsal neurons was not significantly better than chance (accuracy = 0.67 [0.45 0.84]) while decoding based on ventral neurons achieved a significant accuracy (accuracy = 0.83 [0.58 0.93]) (Figure 1E). Moreover, the AUC was 0.64 for the first classifier and 0.82 for the second one. No significant classification of high versus low UPDRS was achieved (accuracy = 0.63 [0.41 0.81]) (Figure 1F).

Decoding results were also robust to the selected partition. Indeed, the decoding performance peaked at a depth-split of 0.6 with an accuracy of 0.91 [0.68 0.97], while for no depth a significant discrimination between patients with high and low UPDRS was achieved.

Discussion

In drugs off condition, the ventral neurons of ICB+ patients display a more regular, less bursty activity than the ventral neurons of ICB- patients. The difference is relevant to the extent that it supports a significant discrimination of the two conditions patient-wise. We previously found that firing regularity was among the markers of ICB+ condition.[13] The novel analysis presented in this manuscript shows that the difference between conditions is localized in the ventral part.

To compare with previous results indicating a role of low frequency LFP in impulsivity,[5–8] we analyzed these bands in the background unit activity. We found that the power associated with these bands was significantly lower in ICB condition in the ventral part of the STN, but not in the dorsal part (LMM, interaction $p < 0.001$). However, the same difference was found when comparing high UPDRS and low UPDRS conditions (LMM, interaction $p < 0.01$). Hence, we could not conclude that milder ventral low frequencies were specifically related to ICB. This conclusion can be drawn only for firing regularity as estimated by the shape factor. A larger dataset will be needed to clarify the role of low frequency components of background activity.

Our results strongly corroborate the growing body of evidence showing that impulsivity is specifically affected by the activity in the ventral part of the STN.[16] Furthermore, our result directly associates a specific ventral STN activity regime with ICB. A higher regularity in STN ventral firing in ICB patients in drugs off condition suggests a candidate explanation for the role of dopamine agonists in favoring ICB onset. At the onset of PD, a minority of

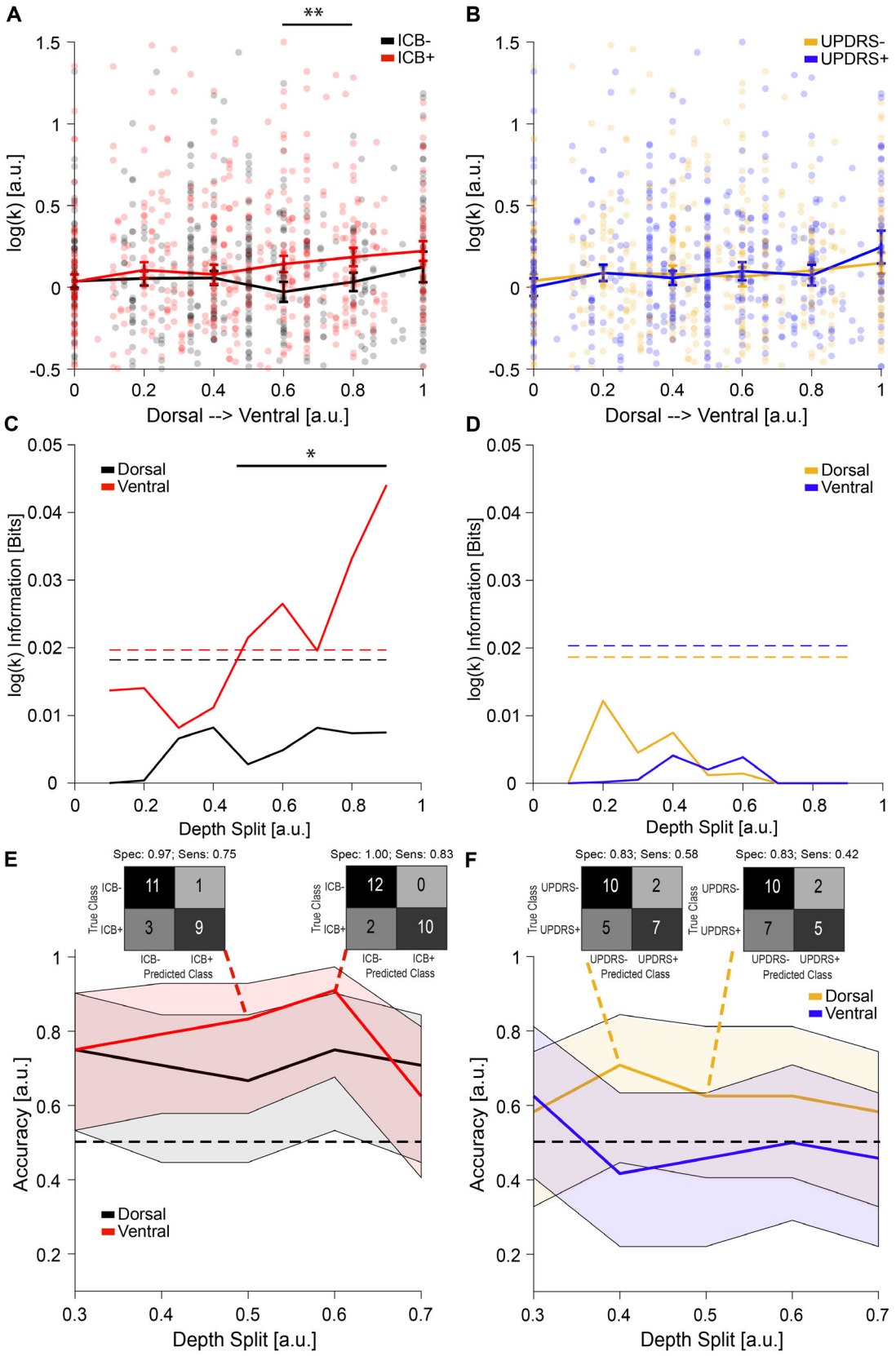

Figure 1. Relation between neural depth and impulsivity discriminative power. (A) Topographical distribution of the neural irregularity as indicated by the shape factor log(k) in ICB+ (black dots) and ICB- patients (red dots) in normalized relative coordinates (STN entry point: 0 and STN exit point: 1). Lines indicate the median and the standard error of median of data in 2 mm bins only for visualization purposes. (B) Same as A for UPDRS- (orange dots and line) and UPDRS+ (blue dots and line) conditions. (C) Cumulative mutual information carried by the irregularity of neurons, starting from the most dorsal border [0 depth] (black line) and most ventral border [depth 1] (red line), about the presence/absence of impulsivity in patients. Dashed lines indicate the significance level (95th percentile) estimated via permutation test. (D) Same as C for discriminating UPDRS- and UPDRS+ conditions starting from the most dorsal border [0 depth] (orange line) and most ventral border [depth 1] (blue line). (E) Decoding performance of neural irregularity in discriminating ICB- and ICB+ patients starting from the most dorsal border [0 depth] (black line) and most ventral border [depth 1] (red line). The shaded area indicates the 95% confidence interval of the accuracy computed via the Clopper–Parson method (*binofit* function in Matlab). The black horizontal line highlights the chance level (0.50 for binary balanced classes). (F) Same as E for classifying UPDRS- and UPDRS+ patients starting from the most dorsal border [0 depth] (orange line) and most ventral border [depth 1] (blue line). Confusion matrices summarize the decoding results at 0.5 depth-split and the local depth-split maximum of performance (0.6 for ICB- vs. ICB+ and 0.4 for UPDRS- and UPDRS+). Asterisks indicate the statistical significance: *p*-value <0.05*, <0.01**, and <0.001***.

patients might have a particularly preserved ventral part activity. For this subset of patients, dopamine agonists, acting non-selectively, might over-compensate in the ventral part, increasing the likelihood of ICB. The methodology introduced here might be applied in future studies i) characterizing the anterior limbic region of the STN by investigating the functional differences along the anterior–posterior axis, and ii) investigating the role of electrode location in post-implant evolution of ICB symptoms.

Acknowledgments

M.V., F.M., and A.M. were supported by internal funds of Scuola Superiore Sant'Anna.

Author Contributions

M.V and F.M. Designed and performed data analysis and wrote the paper. G.P. Collected the data and contributed to write the paper. S.R. Conceived the study, collected the data, and contributed to write the paper. A.M. Conceived the study, designed data analysis, and wrote the paper.

Conflict of Interest

The authors declare no competing interest.

References

1. Baig F, Kelly MJ, Lawton MA, et al. Impulse control disorders in Parkinson disease and RBD: a longitudinal study of severity. Neurology. 2019;93(7):e675-e687.
2. Jahanshahi M, Obeso I, Baunez C, et al. Parkinson's disease, the subthalamic nucleus, inhibition, and impulsivity. Mov Disord. 2015;30(2):128-140.
3. Mazzoni A, Rosa M, Carpaneto J, et al. Subthalamic neural activity patterns anticipate economic risk decisions in gambling. eNeuro. 2018;5(1):e0366-17.2017.
4. Chen W, de Hemptinne C, Miller AM, et al. Prefrontal-subthalamic hyperdirect pathway modulates movement inhibition in humans. Neuron. 2020;106 (4):579-588.e3.
5. Horn A, Neumann W-J, Degen K, et al. Toward an electrophysiological "sweet spot" for deep brain stimulation in the subthalamic nucleus: subcortical mapping of beta band activity in Parkinson's disease. Hum Brain Mapp. 2017;38:3377-3390.
6. Rappel P, Grosberg S, Arkadir D, et al. Theta-alpha oscillations characterize emotional subregion in the human ventral subthalamic nucleus. Mov Disord. 2020;35(2):337-343.
7. Ricciardi L, Fischer P, Mostofi A, et al. Neurophysiological correlates of trait impulsivity in Parkinson's disease. Mov Disord. 2021;36(9):2126-2135.
8. Rodriguez-Oroz MC, López-Azcárate J, Garcia-Garcia D, et al. Involvement of the subthalamic nucleus in impulse control disorders associated with Parkinson's disease. Brain. 2011;134(1):36-49.
9. Ballanger B, van Eimeren T, Moro E, et al. Stimulation of the subthalamic nucleus and impulsivity: release your horses. Ann Neurol. 2009;66(6):817-824.
10. Voon V, Droux F, Morris L, et al. Decisional impulsivity and the associative-limbic subthalamic nucleus in obsessive-compulsive disorder: stimulation and connectivity. Brain J Neurol. 2017;140(2):442-456.
11. van Wouwe NC, Neimat JS, van den Wildenberg WPM, et al. Subthalamic nucleus subregion stimulation modulates inhibitory control. Cereb Cortex Commun. 2020;1(1):tgaa083.
12. Rossi PJ, Shute JB, Opri E, et al. Impulsivity in Parkinson's disease is associated with altered subthalamic but not globus pallidus internus activity. J Neurol Neurosurg Psychiatry. 2017;88(11):968-970.
13. Micheli F, Vissani M, Pecchioli G, et al. Impulsivity markers in parkinsonian subthalamic single-unit activity. Mov Disord. 2021;36(6):1435-1440.

14. Cieciersky K, Mndat T, Rola R, et al. Computer aided subthalamic nucleus (STN) localization during deep brain stimulation (DBS) surgery in Parkinson's patients. Ann Acad Medicae Silesiensis. 2014;68(5):275-283.
15. Vissani M, Cordella R, Micera S, et al. Spatio-temporal structure of single neuron subthalamic activity identifies DBS target for anesthetized Tourette syndrome patients. J Neural Eng. 2019;16(6):066011.
16. Mosher CP, Mamelak AN, Malekmohammadi M, et al. Distinct roles of dorsal and ventral subthalamic neurons in action selection and cancellation. Neuron. 2021;109 (5):869-881.e6.

